Available online at www.sciencedirect.com

ScienceDirect

Procedia CIRP 86 (2019) 126–132

www.elsevier.com/locate/procedia

7th CIRP Global Web Conference
"Towards shifted production value stream patterns through inference of data, models, and technology"

Process design of the patterning process of profile grinding wheels

Denkena, B.[a], Krödel, A.[a], Gartzke, T.[a]*

[a]*Institute of Production Engineering and Machine Tools (IFW), Leibniz Universität Hannover, An der Universität 2, 30823 Garbsen, Germany*

* Corresponding author. Tel.: +49 511 762 18326; fax: +49 511 762 5115. *E-mail address:* gartzke@ifw.uni-hannover.de

Abstract

In production environment, grinding is often the last step along the process chain. At this step, the main share of the value chain is already manufactured. Correspondingly, the process result of this step directly influences the product quality. Thus, the avoidance of process induced damages is a major challenge in grinding. The major limiting factor in grinding is the thermal load on the workpiece, which leads to grinding burn and tensile residual stresses. This thermal load can be reduced, as previous fundamental studies have shown, by means of using microstructured grinding wheels. In this paper, the patterning process of profile grinding wheels is investigated with regard to the resulting geometry and the resulting grinding wheel topography. In detail, an analytical model is established and evaluated that enables a design of the patterning process of profile grinding wheels. The presented formulas describe the local depth and width of a pattern over its length of engagement. The influence of the inclination angle of the patterning tool and the profile angle of the grinding wheel on the resulting width and length of one pattern is investigated. Further influencing parameters on the size of a pattern that are investigated are e.g. the radius of the grinding wheel, the radius of the patterning tool, the corner radius of the patterning edge and the speed ratio between the grinding wheel and the patterning tool. In addition, grinding experiments were conducted to validate the process design. The results show a high correlation between the calculated and the resulting patterns on the grinding wheel as well as that a decrease in cutting forces can be achieved by this approach. When maintaining the workpiece and grinding wheel load, the productivity of the profile grinding process can be increased in this way.

Keywords: Grinding; patterning; structured grinding wheel; dexel simulation; silicon carbide; cast iron

1. Introduction

In manufacturing, grinding is often one of the last steps in the production chain. The process result is therefore directly linked to the product quality. However, grinding with conventional grinding tools is prone to cause thermal induced damage [1]. This damage can be determined by grinding burn or tensile residual stresses [1-6]. Previous studies have shown a correlation between the occurrence of tensile residual stresses and the reduction of the lifetime of a product [7-10].

The thermal load on the workpiece is a result of the process related friction of grains in the contact zone and limited heat flow out of the contact zone. Approaches to reduce the thermal load on the workpiece aim on both, the reduction of friction and the increase of heat flow out of the contact zone. In the case of conventional grinding tools, the shape and material of the grains can be varied to reduce the thermal load, e.g. defined shape of grains or sintered corundum as grain material [3-4]. A further approach is to structure the surface of the grinding wheel. This leads to an increased flow rate of coolant through the contact zone as well as to an increased chip thickness reducing the share of friction in the contact zone [4].

Li and Axinte provided a comprehensive review on the recent developments on structured or textured grinding wheels, which are briefly outlined in this section [11]. In addition, later studies have been conducted by Silva et al. and Zhang et al. [12-13]. The structures are classified based on the size of the structure as well as on the used manufacturing technology. Uhlmann et al. as well as Aurich et al. investigated slotted grinding wheels, which have been structured by means of the manufacturing process of the grinding wheel [5, 14]. Rabiey as well as Göttsching used manufacturing processes such as laser machining or dressing-related processes to structure the grinding wheels [6, 4]. The patterning process, developed by

2212-8271
10.1016/j.procir.2020.01.011

Göttsching, is investigated further in this study. In this process, the grinding wheel is structured by a special form roll in a fly-cutting process, which is kinematically similar to an axis parallel turn milling process (see fig. 1) [2]. The advantage is that the texture dimension is compared to other processes little, which leads to a low increase in roughness of the workpiece surface. The depth of one pattern enabling flexibility as the topography of the grinding wheel can be individually manipulated prior to the grinding process. However, this process is not yet applicable to industrial processes as it is limited to cylindrical, circumferential surfaces of the grinding wheel. Profile grinding wheels cannot be structured, as the process design is not yet developed, which is the primary motivation for this study.

Previous studies on structured grinding wheels focused on the value effective contact area A_{eff}, as a key value for the process design. This describes the active area in relation to the ideal, unstructured surface area (A_{gw}) and is given by eq. 1 [2,6]. In this, A_p is the passive area, which is removed off of the grinding wheel surface by the structuring process. For patterning processes with repeating patterns, the passive area can be calculated by the number of patterns N_p and the area of one pattern A_μ (see eq. 2). The number of patterns is a result of the rotational speed ratio λ between the patterning tool and the grinding wheel, the number of cutting edges N_{dia}, the axil feed rate f and the width of patterned surface b_{gw}.

$$A_{eff} = \left(1 - \frac{A_p}{A_{gw}}\right) \cdot 100\% \quad (1)$$

$$A_p = N_p \cdot A_\mu \quad (2)$$

$$N_p = \lambda \cdot N_{dia} \cdot \frac{b_{gw}}{f} \quad (3)$$

Eq. 1-3 show that A_μ is a highly important value for the process design. Regarding the structuring of profile grinding wheels, an interaction between the structuring tool inclination angles and the value of A_μ is expected. Therefore, a dedicated investigation of this influence is necessary. The other values consist of setting parameters, which can be adjusted with a high accuracy in grinding.

2. Material and methods

The process design in this study was calculated mainly using an analytical approach. As a result, an analytical model was established. In addition, numerical calculations were conducted to validate the analytical approach. This was done as the analytical model included simplifications. Moreover, the developed process design method was applied to SiC profile grinding wheels to validate the process design within a grinding application.

2.1 Simulation setup

The numerical calculation was conducted via the dexel-based material removal simulation software IFW CutS. Within this software a model was developed, which includes an unstructured grinding wheel and the patterning tool. Both, the grinding wheel and the patterning tool, are established as simplified bodies in order to reduce the computing effort. Fig. 1 depicts this model with the relevant kinematics on the right side. The grinding wheel is modelled by dexels, which can be shortened when having contact with the patterning tool. The patterning tool is modelled as a surface mesh. The kinematical fundamentals of the analytical model are shown in Fig. 1 on the left side.

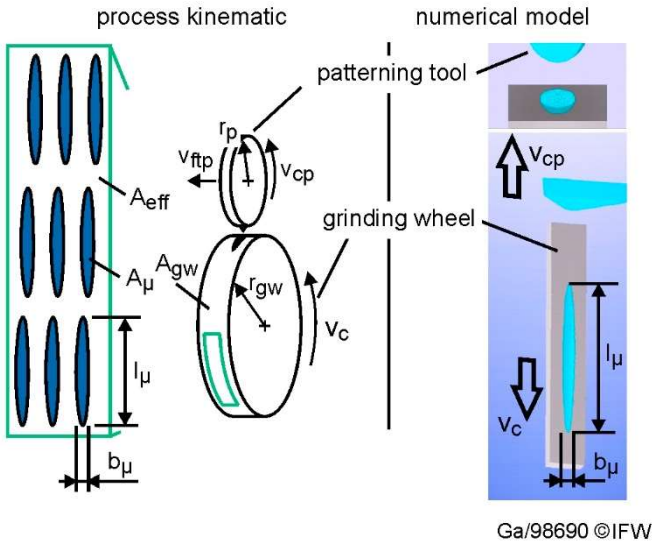

Figure 1. Analytical (left) and numerical approach (right) with relevant process setting parameters of the patterning process

The resolution of the dexel model was 2 µm. The resolution of time was 0.1 ms, while the total cutting time for one pattern was approx. 470 ms. This resolution resulted in a total error of < 10 µm for the length of a pattern. As the length of a pattern is in average 4.5 mm, the error is below 1%. The error in width and area of a pattern is smaller as the time resolution has no influence on this.

2.2 Experimental setup

Throughout the experimental investigation, the patterning process is applied to a grinding process, in which samples of GJS700 are ground on a continuous gear grinding machine KAPP KX 1. This machine enables a high accuracy in revolution per minute of both, the main spindle and the dressing tool spindle, leading to an increased quality of the patterning process. The corresponding experimental setup is displayed in Fig. 2. The patterning tool is a custom-made tool from Dr. Kaiser GmbH with a single pocket for indexable inserts. The inserts have a thick layer chemical vapour deposition diamond (CVD-D) brazed on a tungsten carbide carrier as a cutting material. The dimensions are TNXX0X0350 with an edge radius r_ε of 0.5 mm. The dressing spindle is a C 80 FAW from Dr. Kaiser GmbH and has a working range of 1 to 3000 rpm. It is positioned on a jig that enables an inclination movement, which is needed to pattern the front face of the grinding wheel. The patterns were machined with a depth of a_{ep} = 60 µm.

The grinding wheels are vitrified bonded green silicon carbide (SiC) from Krebs & Riedel Schleifscheibenfabrik GmbH & Co. KG in the specification 200x30x127 A 57C, with a varied mesh size of #60 and #120.

For the test, the grinding wheel is dressed on the circumferential and the face side with an overlapping ratio U_d = 4, a dressing depth of cut a_{ed} = 5 µm for 20 times. Subsequently, the total depth of cut is 100 µm, which is chosen to remove the patterns of the previous experiment. The dressing operation is conducted with a multi grain dresser (M/100) from Jakob Lach-Diamant GmbH & Co. KG.

The grinding process is conducted on a workpiece with a pre-machined profile, as shown in fig. 2, with a depth of 4 mm. The process parameters are a_e = 0.5 mm, a_p = 15 mm, v_c = 20 m/s, 2 strokes. The length of the sample is 40 mm.

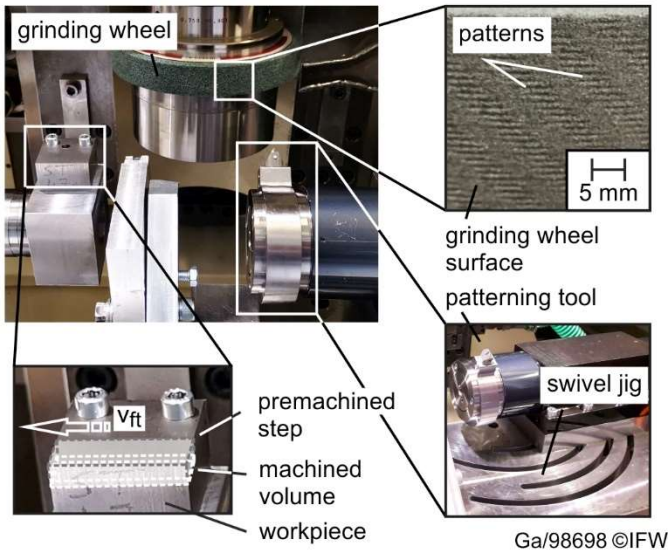

Figure 2. Experimental setup for the grinding process

In regard to the accuracy of the patterning process, the engagement width was measured with a Keyence microscope VHX-600 prior to the patterning test. The further measurement equipment consisted of 4 Kistler force measurement components 9018A, which are positioned under the workpiece clamping unit.

3. Modelling of the patterning process

The patterning process of this study is conducted with a fly-cutting kinematic. As outlined in the introduction, the effective contact area is a key value when machining with patterned grinding wheels. This value is highly influenced by the size of one pattern. In previous studies, this area has been evaluated by the length and width of a pattern and the assumption that the shape of the pattern is similar to an ellipse. Furthermore, it is not yet possible to calculate these values when patterning profile grinding wheels, as the inclination angle of the patterning tool as well as the profile angle of the grinding wheel were neglected in existing research. To enable the process design, the length, the width and the area of the resulting patterns are modelled in the following section.

3.1 Length of a pattern

The length of a pattern l_μ can be analytically described as the engagement length of the patterning tool and the grinding wheel. To calculate this engagement, the movement of the patterning tool has to be modelled in relation to the grinding wheel surface. This movement can be described as a cycloid. According to Schulz [15], the engagement can be expressed by the following eq. 4, while ± is dependent on the direction of cut (+: counter direction; -: concurrent direction). The value q_d is the dressing speed ratio. This equation underlies the simplification of a linearised grinding wheel surface, which is compensated by the use of an equivalent dressing tool diameter d_{eqp}. This value is defined by eq. 5, in which r_{gw} is the radius of the grinding wheel and r_p the radius of the patterning tool. Fig. 3 illustrates this, including the coordinates x, y and z.

$$x = \sqrt{y \cdot d_{eqp}} \cdot \left(\frac{1}{|q_d|} \pm 1\right) \quad (4)$$

$$d_{eqp} = 2 \cdot \frac{r_{gw} \cdot r_p}{(r_{gw} + r_p)} \quad (5)$$

The resulting engagement length is calculated for the maximum depth of engagement ($y = a_{ep}$). As eq. 4 describes the half of the engagement length, the length of a pattern l_μ can be analytically described by the eq. 6. In this, the arithmetic expression "((1/|q_d|)± 1)" describes a factor by which a base length l_0 is prolonged or compressed due to the relative movement of the patterning edge and the grinding wheel during the engagement. In the case of patterning, it can be replaced by the expression (1 ± (1/|q_d|)) to express the modulus. This replacement is reasonable as it prevents the calculation of negative pattern lengths. It corresponds to the prolonging factor of the calculation of Göttsching [18]. The base length describes the plain geometrical intersection of the enveloping surfaces of the grinding wheel and the patterning tool [8].

$$l_\mu = 2 \cdot \sqrt{a_{ep} \cdot d_{eqp}} \cdot \left(1 \pm \frac{1}{|q_d|}\right) = l_0 \cdot \left(1 \pm \frac{1}{|q_d|}\right) \quad (6)$$

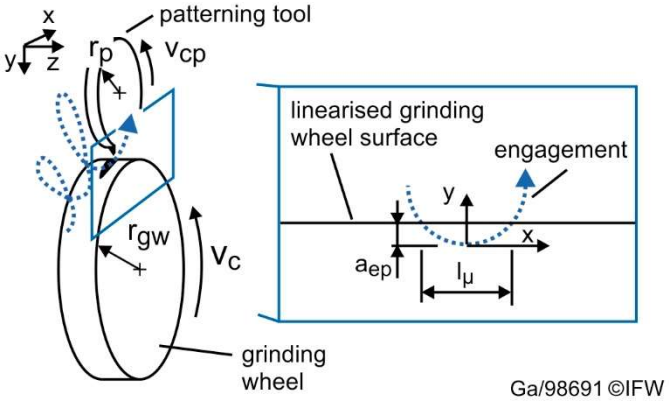

Figure 3. Model of engagement of patterning tool into linearised grinding wheel surface

Eq. 4 and 6 are valid for an engagement with a kinematic of parallel axes of the patterning tool and the grinding wheel. Since profile grinding wheels are investigated in this study, two further angles have to be introduced. Firstly, the profile angle φ describes the angle at which the surface of the grinding wheel is tilted against the central line of the grinding wheel (see fig. 4 left side). It is defined that the patterning tool engages in surface normal direction. Secondly, the inclination angle Θ describes the inclination of the patterning tool against the surface normal direction, i.e. the angle between the axis of the patterning tool and the profile angle. The influence of φ and Θ on the length of a pattern can therefore be calculated by their influence on the base length, i.e. the geometrical intersection of the grinding wheel and the patterning tool. This intersection is, in the case of the circumferential patterning process, an intersection of two circles. However, when adding the angles φ and Θ the circles are distorted. As the length of the pattern is defined in the circumferential direction, the circle that describes the circumference of the patterning tool has to be projected onto in the surface normal plane of the grinding wheel. The result is an ellipse with an unchanged semi-major axis of r_p and a shortened semi-minor axis that is expressed by

eq. 8. This relation is similar in the case of the profile angle φ and is given by eq. 9:

$$r_{p,\Theta} = r_p \cdot \cos(\Theta) \quad (8)$$

$$r_{gw,\varphi} = r_{gw} \cdot \cos(\varphi) \quad (9)$$

As previously outlined, the base length can be calculated by the length between the two points of intersection. Therefore, the equations for the ellipses have to be established and the points of intersection have to be calculated. Based on the geometrical assumptions in fig. 4 (right) and eq. 8-9, equations 10 and 11 can be established. The variable k is introduced for visualisation purposes.

$$1 = \frac{x^2}{{r_{gw}}^2} + \frac{y^2}{{r_{gw,\varphi}}^2} \quad (10)$$

$$1 = \frac{x^2}{{r_p}^2} + \frac{(y-k)^2}{{r_{p,\Theta}}^2} \quad (11)$$

$$k = r_{gw,\varphi} + r_{p,\theta} - a_{ep}$$

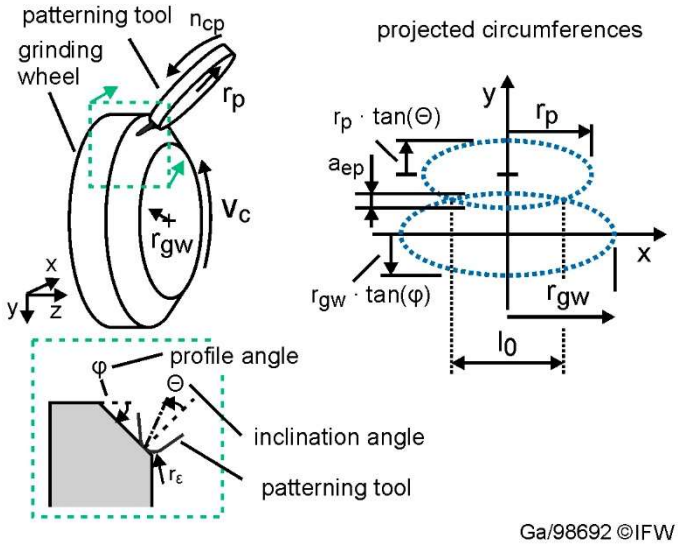

Figure 4. Definition of profile and inclination angle with influence on the projected circumferences and the base length l_0

For the points of intersection, the difference of eq. 10 and eq. 11 has to be zero. This results after repositioning in the eq. 12:

$$0 = r_{gw}^2 - \frac{r_{gw}^2}{r_{gw,\varphi}^2} \cdot y^2 - r_p^2 + \frac{r_p^2}{r_{p,\Theta}^2} \cdot (y-k)^2 \quad (12)$$

The zeros of eq. 12 can be solved by using the pq-formula. However, only the negative zero is a realistic solution for the application of patterning. In general, two ellipses can have four points of intersection, which are calculated out of the zeros. This is not the case in this application. The resulting zero is outlined in eq. 13:

$$y_0 = \frac{(r_p^2 \cdot k \cdot r_{gw,\varphi}^2) - \sqrt{A}}{r_p^2 \cdot r_{gw,\varphi}^2 - r_{gw}^2 \cdot r_{p,\Theta}^2} \quad \text{with} \quad (13)$$

$$A = r_p^4 \cdot r_{gw,\varphi}^4 \cdot k^2 + r_{gw,\varphi}^2 \cdot (r_{gw}^2 \cdot r_{p,\Theta}^2 - r_p^2 \cdot r_{p,\Theta}^2 + r_p^2 \cdot k^2) \cdot (r_{gw}^2 \cdot r_{p,\Theta}^2 - r_p^2 \cdot r_{gw,\varphi}^2)$$

When entering y_0 into eq. 10, the x-value of the point of intersection can be calculated. Due to the symmetry, the distance between the two points, i.e. the base length l_0, can be calculated as the double:

$$l_0 = 2 \cdot x_0 = 2 \cdot \frac{r_{gw}}{r_{gw,\varphi}} \cdot \sqrt{r_{gw,\varphi}^2 - y_0^2} \quad (14)$$

With eq. 7, 13 and 14, it is possible to calculate the length of a pattern under the influence of the profile angle φ and the inclination angle Θ.

3.2 Width of a pattern

Similar to the length l_μ, the width of a pattern b_μ is the result of the engagement of the patterning tool with the surface of the grinding wheel. To calculate this, the local depth within the pattern y(x) is calculated. This is done by the use of eq. 4. This equation needs to be repositioned and reflected as well as the the maximum depth of cut needs to be added. The result is shown in eq. 15.

$$y(x) = -\frac{x^2}{d_{peq} \cdot \left(\frac{1}{|q|} \pm 1\right)^2} + a_{ep} \quad (15)$$

Then, the local width of a pattern can be modelled by the use of functions describing the geometrical shape of the patterning cutting edge. The width as a function of the local depth of cut is modelled in this study for a round and a triangle shape, which are common shapes for patterning tools. The functions that describe the outer line of the pattern, i.e. half of the width of the pattern, can be expressed by eq. 16 and 17. Eq. 16 is the function of the width machined by a round cutting edge z_{ci} (x). It is based on the length of a secant. Eq. 17 is the function of the width machined by a triangle shaped edge z_{tr} (x), in which ε is the corner angle. Both equations are based on the assumption that small engagement angles are negligible. The length of a pattern is modelled in a similar way. Fig. 5 illustrates the results of eq. 16 and 17 on common patterning parameters.

$$z_{ci}(x) = \sqrt{2 \cdot r_\varepsilon \cdot y(x) - y(x)^2} \quad (16)$$

$$z_{tr}(x) = y(x) \cdot \tan\left(\frac{\varepsilon}{2}\right) \quad (17)$$

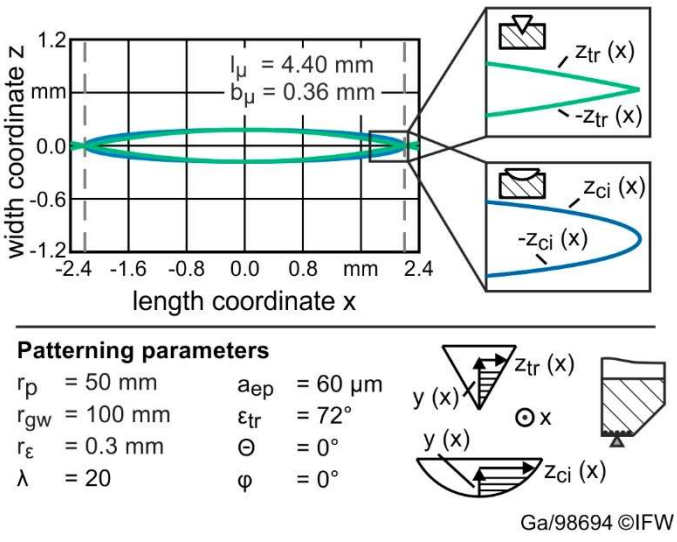

Figure 5. Engagement widths of z_{ci} (x) and z_{tr} (x) and their reflected functions

As for the length of a pattern, eq. 15-17 are valid for a parallel position of the axes. To determine the influence of the profile angle and the inclination angle on the width of a pattern, the maximum width b_μ is further investigated. In the case of a triangle shaped edge, eq. 17 is extended to the form of eq. 18, to which the inclination angle is added. Equation 18 also takes both sides of the engagement and the maximum depth of cut a_{ep} into account.

$$b_{\mu,tr} = a_{ep} \cdot \left(\tan\left(\frac{\varepsilon}{2} + \Theta\right) + \tan\left(\frac{\varepsilon}{2} - \Theta\right)\right) \quad (18)$$

For a round corner condition, the inclination of the tool can lead to an engagement of the straight part of the cutting edge. Therefore, a case differentiation is done as follows for which a value y_{crit} is introduced. This value describes the distance from the point of maximum depth to the beginning of the straight part of the edge in direction of the depth of cut and is expressed by eq. 19.

$$y_{crit} = r_\varepsilon \cdot \left(1 - \sin\left(\frac{\varepsilon}{2} + \Theta\right)\right) \quad (19)$$

With this value and geometrical considerations the following case differentiation can be done. Herein, eq. 20 is the double of eq. 16 describing both sides of engagement with a full round corner. Out of geometrical considerations eq. 21 describes the width of cut if one straight part of the edge engages:

$$y_{crit} \geq a_{ep}: \quad b_{\mu,ci} = 2 \cdot \sqrt{2 \cdot r_\varepsilon \cdot a_{ep} - a_{ep}^2} \quad (20)$$

$$y_{crit} < a_{ep}: \quad b_{\mu,ci} = \sqrt{2 \cdot r_\varepsilon \cdot a_{ep} - a_{ep}{}^2} + \sqrt{2 \cdot r_\varepsilon \cdot y_{crit} - y_{crit}{}^2} + (a_{ep} - y_{crit}) \cdot \tan\left(\frac{\varepsilon}{2} + \Theta\right) \quad (21)$$

The inclination angle for which $y_{crit} = a_{ep}$ is named Θ_{crit}. This relation is depicted in fig. 6 on the left side. On the right side, results for common patterning parameters are shown. It can be seen that the inclination has no influence on the width of a pattern if $\Theta < \Theta_{crit}$. It can also be seen that the r_p is mainly determining the width for constant depths of cut.

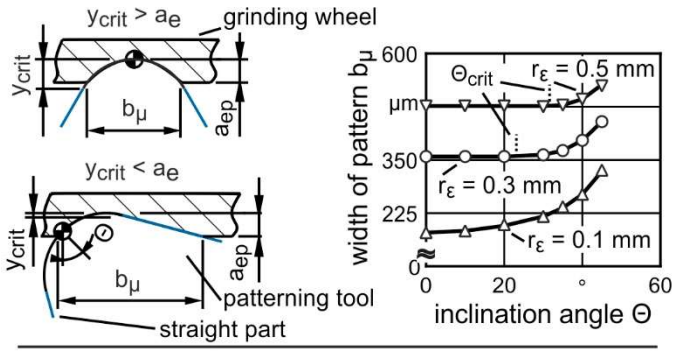

Patterning parameters

r_p	= 50 mm	a_{ep}	= 60 µm
r_{gw}	= 100 mm	ε	= 60°
r_ε	= 0.1, 0.3, 0.5 mm	Θ	= 0 - 45°
λ	= 20	φ	= 0°

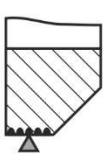

Ga/98695 ©IFW

Figure 6. Influence of the inclination angle on the resulting width of a pattern

However, for the profile angle there is no influence on the width of a pattern. Reason for this is the patterning tool is not tilted against the normal direction of the surface. Therefore, the maximum width is sufficiently modelled by eq. 18-21.

3.3 Area of a pattern

In previous studies, the area of a pattern was calculated by the formula of an ellipse [8]:

$$A_\mu = \frac{1}{4} \cdot \pi \cdot l_\mu \cdot b_\mu \quad (22)$$

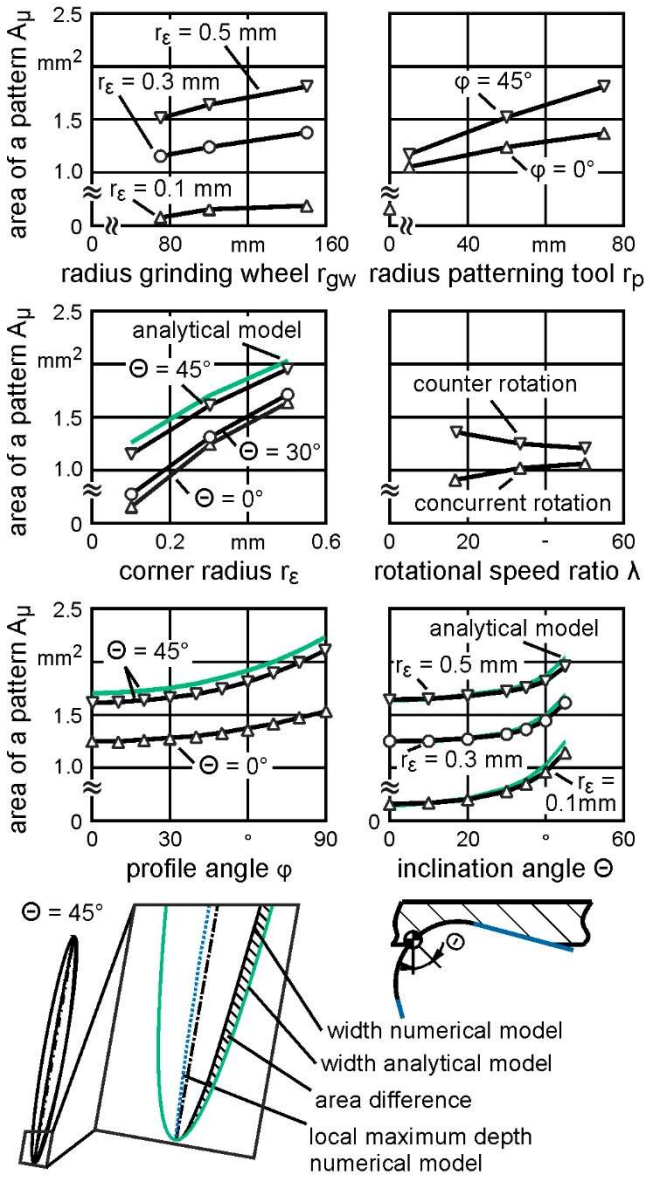

Patterning parameters

r_p	= 25, 50, 75 mm	a_{ep}	= 60 µm
r_{gw}	= 75, 100, 150 mm	ε	= 60°
r_ε	= 0.1, 0.3, 0.5 mm	Θ	= 0 - 45°
λ	= 10, 20, 30	φ	= 0 - 90°

(x: value if not stated differently)

Simulation Software

IFW CutS

dexel-based Material-removal Simulation

Ga/98696 ©IFW

Figure 7. Results of the numerical model in comparison to the corresponding results of the analytical model

However, the results of chapter 3.2 show that this is not valid in all cases. Especially, the engagement with triangle shaped cutting insert leads to a different pattern shape. A way to achieve a more accurate result is by the integrals of eq. 18-19. However, in regard to the simplifications of an analytical calculation as well as the implemented angles φ and Θ, a numerical model is established to model the resulting area. Furthermore, the results are compared to the results using eq. 4-22.

The results are shown in fig. 7, in which the numerical results are shown (black with dots) in comparison to the analytical results (green). The results of the analytical model are not displayed, if the error is below 3 %. In most cases, the patterns are sufficiently modelled by eq. 4-22. Even though, a difference can be observed for the influence of the inclination angle and in the case of a corner radii of 0.1 mm. In both cases, the straight part of the cutting edge engages leading to a change in pattern shape compared to the shape of eq. 22. However, this error was within the investigated parameter setup below 10%. Therefore, the analytical model can be used for the process design, which enables a universal application.

For an applicable process design, the effective contact area A_{eff} is of interest as previous studies have determined the influence of this value on the grinding process [8, 15]. Thus, the value of A_{μ} is used in combination with eq. 1-3 to design the patterning process.

4. Experimental investigation

Within the experimental part of this study, two different grinding wheels were patterned with 2 different effective contact areas and compared to an unpatterned grinding wheel (see fig. 2). In the middle of fig. 8, the patterned grinding wheel with #120 is shown. The resulting patterns are depicted . Furthermore, the grinding forces are also illustrated in this figure. The grinding forces are increasing with the relative material removal rate Q'_w. However, the forces are reduced by an increase in grain size as well as by the patterns. In both cases, the chip thickness is increased, which leads to a reduction in friction. Subsequently, the patterning process can increase the relative material removal rate, while maintaining the forces.

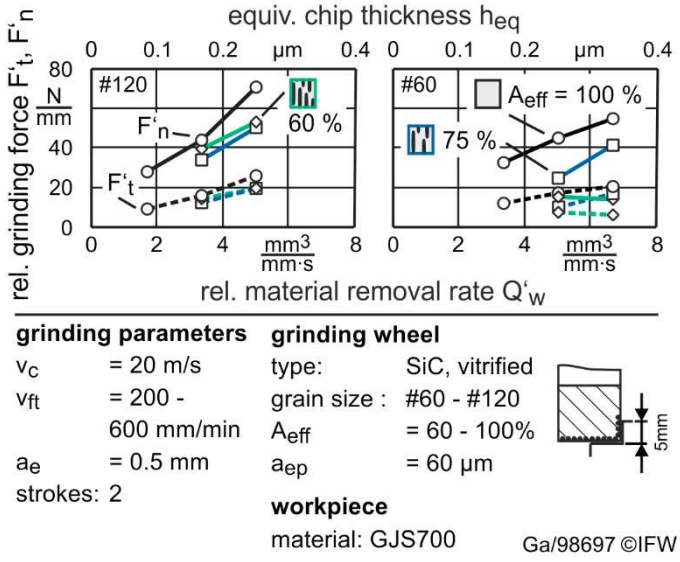

Figure 8. Influence of the patterns on the resulting grinding forces.

In this study, the influence of the patterns on the grinding process increases with increasing grain size. The forces are reduced by max. 25 % by the patterns for the grain size #120, whereas the forces are reduced by 74 % for the grain size #60. This can also be explained by the chip thickness. The influence of the patterns on the grinding process is due to a reduction of friction of the grains in the contact zone. This is achieved by an increase of chip thickness. However, this effect appears not to be global but local behind a pattern. The chip thickness increases due to the interruption of cut. Subsequently, the ratio of number of grains in the contact zone and the number of patterns determines the ability to influence the effect of patterns on grinding processes.

5. Conclusion and outlook

The design of the patterning process of vitrified grinding wheels for profile grinding applications was established in this paper. Therefore, the length, width and area of a resulting pattern are modelled analytically by the engagement of the patterning tool with the grinding wheel. Influencing factors on the geometrical extension of the pattern are:

- Radii of grinding wheel, patterning tool and corner of the patterning edge
- The rotational speed ratio between the grinding wheel and the patterning tool
- The inclination angle of patterning tool against the surface normal of the grinding wheel
- The profile angle of the grinding wheel

It was possible to validate the analytical model, especially with regard to its simplifications , by a comparison of the established analytical model and a numerical model. The advantage of the analytical model is the low computational effort required for the process design of individual applications. The reason for this is that this model is universally applicable, while the numerical model has to be modelled for each case new. Limitations of the analytical model, caused by the engagement of the straight part of the cutting edge, were shown by the calculation of the width of a pattern. If this part is engaging, the resulting shape of a pattern differs from an ellipse. This is of particular importance when applying an inclination angle to the patterning process.

The process design was validated by the experimental investigation. The grinding forces are reduced when grinding with patterned grinding wheels. In addition, the influence of the patterns on the grinding process increases with increasing grain size of the grinding wheel. A possible explanation for this is the ratio of the number of grains and the number of patterns, as the reason for the reduced grinding forces is determined by an increase in chip thickness. This hypothesis is due to be investigated in further studies including an investigation on the material removal mechanisms.

Acknowledgements

The authors would like to thank the Federal Ministry for Economic Affairs and Energy (BMWi) Germany for their organizational and financial support within the project “Improvement in performance of vitrified bonded corundum

grinding wheels for profile creep feed grinding" with the funding number "IGF 19414 N/1".

References

[1] Hoffmeister, H.-W., Hahmann, W.-C.: Innovative Ansätze für das Kühlen beim Schleifen, In: Tawakoli, T. (ed.): Moderne Schleiftechnologie und Feinstbearbeitung 2012, 9th Seminar, Villingen-Schwenningen, pp. 7-1 – 7-20., 2012

[2] Denkena, B., Grove, T., Göttsching, T.: „Grinding with patterned grinding wheels", CIRP Journal of Manufacturing Science and Technology 8, pp. 12-21, 2015

[3] Wegener, K., Bleicher, F. Krajnik, P., Hoffmeister, H.-W., Brecher, C.: Recent developments in grinding machines, CIRP Annals – Manufacturing Technology, Vol. 66, pp. 779-802, 2017

[4] Göttsching, T.C.: Schleifen von aluminiumhaltigem UHC-Stahl, Dr.-Ing. Dissertation, University Hannover, 2017

[5] Tawakoli, T., Amir, D.: Innovative Abrichtrolle mit Punktkontakt optimiert die Abrichtprozesse, T-Dress, In: Tawakoli, T. (ed.): Moderne Schleiftechnologie und Feinstbearbeitung 2012, 9th Seminar, Villingen-Schwenningen, pp. 4a1–4a21, 2012

[6] Rabiey, M.: „Dry Grinding with CBN Wheels, The Effect of Structuring", Dr.-Ing. Dissertation, University Stuttgart, 2010

[7] Denkena, B., Poll, G., Maiß, O., Neubauer, T.: Affecting the Life Time of Roller Bearings by an Optimal Surface Integrity Design After Hard Turning and Deep Rolling, Advanced Materials Research Vols. 966-967, pp. 425-434, 2014

[8] Denkena, B., Grove, T., Maiß, O., Neubauer, T., Poll, G., Dreier, S.: Increasing the lifetime of roller bearings by using precision deep rolling, euspen's 15th International Conference & Exhibition, Leuven, Belgium, 2015

[9] Maiß, O.: Lebensdauererhöhung von Wälzlagern durch mechanische Bearbeitung, Dr.-Ing. Dissertation, University Hannover, 2019

[10] Hacke, B., Radnai, B., Hinkelmann, K.: Berücksichtigung von Betriebszuständen, Sonderereignissen und Überlasten bei der Berechnung der Wälzlager-Lebensdauer in Windenergieanlagen und Großgetrieben, Final Report FVA Research Project Nr. 541, Booklet Nr. 967, 2010, AiF-Nr. 15227 N

[11] Li, H.N., Axinte, D.: „Textured grinding Wheels: A review", International Journal of Machine Tools & Manufacture, Vol. 109, pp. 8-35, 2016

[12] Silva, E.J. da, Marcos, G.P., Venter, G.S., Bottene, A.C., Oliveira, J.F.G. de, Rodrigues, C.A.: Development of a patterning system for vitrified CBN wheels based on modal analysis, CIRP Annals – Manufacturing Technology, Vol. 67, pp. 341-344, 2018

[13] Zhang, X., Zhang, Z., Deng, Zr. Wu, Q., Kang, Z.: Precision grinding of silicon nitride ceramic with laser macro-structured diamond wheels, Optics & Laser Technology, Vol. 109, pp. 418-428, 2019

[14] Uhlmann, E., Hochschild, L.: Tool optimization for high speed grinding, Production Engineering – Research and Development, Vol. 7, pp. 185-193, 2013

[15] Schulze, A.: Das Abrichten von keramisch gebundenen CBN-Schleifscheiben mit Formrollen, Dr.-Ing. Dissertation, RWTH Aachen, 1997